Biochimica et Biophysica Acta 1864 (2016) 1292–1303

Contents lists available at ScienceDirect

Biochimica et Biophysica Acta

journal homepage: www.elsevier.com/locate/bbapap

Diverse cap-binding properties of *Drosophila* eIF4E isoforms

Joanna Zuberek [a,*,1], Krzysztof Kuchta [b,c,1], Greco Hernández [d], Nahum Sonenberg [e], Krzysztof Ginalski [b]

[a] Division of Biophysics, Institute of Experimental Physics, Faculty of Physics, University of Warsaw, Warsaw 02-089, Poland
[b] Laboratory of Bioinformatics and Systems Biology, Centre of New Technologies, University of Warsaw, Warsaw 02-097, Poland
[c] College of Inter-Faculty Individual Studies in Mathematics and Natural Sciences, University of Warsaw, Warsaw 02-089, Poland
[d] Division of Basic Research, National Institute of Cancer (INCan), Tlalpan, Mexico City 14080, Mexico
[e] Department of Biochemistry and Goodman Cancer Research Centre, McGill University, Montreal, QC H3A 1A3, Canada

ARTICLE INFO

Article history:
Received 7 June 2016
Accepted 28 June 2016
Available online 29 June 2016

Keywords:
eIF4E family
Translation initiation
Cap analogues
Protein-ligand interactions
Fluorescence spectroscopy

ABSTRACT

The majority of eukaryotic mRNAs are translated in a cap-dependent manner, which requires recognition of the mRNA 5′ cap by eIF4E protein. Multiple eIF4E family members have been identified in most eukaryotic organisms. *Drosophila melanogaster* (*Dm*) has eight eIF4E related proteins; seven of them belong to Class I and one to Class II. Their biological roles with the exception of *Dm* eIF4E-1, *Dm* eIF4E-3 and *Dm* 4EHP, remain unknown. Here, we compare the molecular basis of *Dm* eIF4E's interactions with cap and eIF4G peptide by using homology modelling and fluorescence binding assays with various cap analogues. We found that despite the presence of conserved key residues responsible for cap recognition, the differences in binding different cap analogues among Class I *Dm* eIF4E isoforms are up to 14-fold. The highest affinity for cap analogues was observed for *Dm* eIF4E-3. We suggest that *Dm* eIF4E-3 and *Dm* eIF4E-5 bind the second nucleoside of the cap in an unusual manner *via* stacking interactions with a histidine or a phenylalanine residue, respectively. Moreover, the analysis of ternary complexes of eIF4G peptide–eIF4E–cap analogue showed cooperativity between eIF4G and cap binding only for *Dm* eIF4E-4, which exhibits the lowest affinity for cap analogues among all *Dm* eIF4Es.

1. Introduction

Post-transcriptional regulation of gene expression plays a key role in many cellular and developmental processes. In eukaryotes, the vast majority of mRNAs are translated via the cap-dependent mechanism, in which the cap binding protein eIF4E, complexed with a scaffold protein eIF4G, binds the cap structure (m^7GpppN, where N is any nucleotide) at the 5′ end of the mRNA to recruit the small ribosomal subunit to initiate translation. In this mechanism, cap recognition by eIF4E, as well as the formation of the eIF4E–eIF4G complex, are two of the limiting steps regulating the global process of translation [1,2]. eIF4E is negatively regulated by eIF4E-binding proteins (4E-BP), which share with eIF4G the canonical eIF4E-binding motif (C-motif) YXXXXLϕ (where X is any amino acid and ϕ is a hydrophobic residue) that interacts with the convex dorsal surface of eIF4E. Binding of 4E-BPs to eIF4E precludes formation of the eIF4E–eIF4G complex, thereby repressing cap-dependent translation [3,4].

With the advent of genome-wide sequencing projects of hundreds of organisms across disparate *phyla*, a number of eIF4E genes have been discovered and classified into three Classes [5,6]. Interestingly, some species have been reported to have several eIF4E paralogues that display different expression patterns in certain tissues, promote or inhibit translation of specific mRNAs, are involved in translation under stress responses, or show variable biochemical properties. Moreover, some eIF4E orthologues are also restricted to specific phylogenetic lineages [5–13]. Mammalians have four eIF4E isoforms, eIF4E (also called eIF4E-1a), eIF4E-1b belonging to Class I, eIF4E-2 (or 4EHP) belonging to Class II and eIF4E-3 belonging to Class III. Whereas eIF4E-1a is the major translation factor, eIF4E-2 acts in a cell most probably as a translation repressor. It has been shown that mouse 4EHP binding homeodomain transcription factor Prep1 inhibits *Hoxb4* translation [14] and, along with Grb10-interacting GYF protein (GIGYF2) and zinc finger protein 598, it is a member of translational repressor complex during embryonic development [15]. However, some recent studies [16–18] have indicated an alternative role for 4EHP. They showed that under conditions of extreme oxygen depletion (hypoxia), human cells use 4EHP in the process of an alternative cap-dependent translation. The findings concerning the role of eIF4E-3, the fourth member of mammalian eIF4E family, suggest that it acts as a tissue-specific tumour suppressor [19]. The biological role of eIF4E-1b in mammalian cells remains unknown. The expression of this isoform is strictly limited to oocytes across all classes of *Tetrapoda* [9]. Its role was identified in *Xenopus* oocyte, were it is member of CPEB mRNP repressor complex [20].

* Corresponding author.
E-mail addresses: jzuberek@biogeo.uw.edu.pl (J. Zuberek), kuchtak@cent.uw.edu.pl (K. Kuchta), greco.hernandez@gmail.com (G. Hernández), nahum.sonenberg@mcgill.ca (N. Sonenberg), kginal@cent.uw.edu.pl (K. Ginalski).
[1] These authors contributed equally to the paper as first authors.

http://dx.doi.org/10.1016/j.bbapap.2016.06.015
1570-9639/

The biological role of eIF4E family members has been also extensively investigated in a nematode, *Caenorhabditis elegans*, encoding five eIF4E family members (IFE-1 to -5) [13,21], which show different expression patterns and effects of gene deletion and mutations for growth and development. The IFE-3 isoform, which is closely related to mammalian eIF4E-1a, is essential for viability and embryogenesis [13] and it regulates sex-determination in the hermaphrodite germline [22]. IFE-1, which is expressed in germ-line along with IFE-3 and IFE-5, is required for production of functional sperm, as it affects the expression of some sperm-specific proteins, such as GSP-3 and MSPs [23,24]. IFE-2, which also functions in germline, is mostly expressed in somatic tissues [13]; knock-out of the *ife-2* gene reduces somatic mRNA translation. IFE-4, the only one *C. elegans* eIF4E isoform belonging to Class II, is enriched in soma and its loss produces a pleiotropic phenotype inducing a defect in egg-laying by reducing translation IFE-4 sensitive mRNA [25].

Another species with several eIF4E genes *is Drosophila melanogaster*, a model organism that has provided extensive insight into post-transcriptional mechanisms for regulating gene expression. It contains seven genes encoding eight eIF4E paralogues, namely *Dm* eIF4E-1, -2, -3, -4, -5, -6, and -7 belonging to Class I, and *Dm* 4EHP belonging to Class II. The expression of these proteins varies throughout the development [26,27]. For some of them, a tissue-specific role has been reported. Whereas eIF4E-1 is ubiquitous and required for general translation in all tissues [5,26], eIF4E-3 is a testis-specific protein required only for spermatogenesis [28,29], and 4EHP is a translational repressor that inhibits translation of specific mRNAs during early embryogenesis [30–32]. Despite these few cases, the biological roles played by the majority of the eIF4E-related proteins, as well as their structural and biochemical properties, remain unknown.

The structures of several eIF4E family proteins from different species in the *apo* form, and either in binary or ternary complex with various cap analogues and a fragment of eIF4G or a 4E-BP that contain the eIF4E-binding site, have been solved [33–39]. The eIF4E-like fold is characterised by the presence of an eight-stranded antiparallel β-sheet backed by α-helices (with β1β2α1β3β4α2β5β6α3β7α4β8 topology, as observed in mouse eIF4E (PDB: 1EJ1) [33]), forming a structure described as a cupped hand [33]. These studies have demonstrated that eIF4G or 4E-BP proteins bind to the dorsal surface of eIF4E via a canonical motif (C-motif) and as shown recently for some 4E-BPs, by a non-canonical motif (NC-motif) to a lateral surface of eIF4E [37–39]. On the other side, they have shown that cap nucleotides interact with a narrow slot on the concave surface of eIF4E. The interatomic contacts between eIF4E proteins and cap analogues can be divided into three classes: (i) sandwiching of the 7-methyl guanine between two tryptophan residues (in Class I eIF4E isoforms) or a tryptophan and a tyrosine residues (in Class II); (ii) hydrogen bonds and van der Walls contacts with the 7-methylguanosine; and (iii) direct interactions and water-mediated contacts with the phosphate chains of a cap structure and a positively charged pocket of the cap-binding slot of eIF4E formed by the side chains of several Lys and Arg residues [12,33,35].

Although all members from each eIF4E multigenic family are structurally- and sequence-related proteins, we need to understand the features of various eIF4Es that account for their differences in activity and regulation. Here, using biophysical methods, we characterise the structural properties of all eIF4E paralogues from *D. melanogaster* (*Dm* eIF4Es) both, in a binary complex with diverse cap analogues, and in a ternary complex with cap analogues and the eIF4G C-motif.

2. Material and methods

2.1. Synthesis of cap analogues

Mono- and dinucleotide cap analogues were synthesised as described previously [40–42]. Cap analogues concentrations were determined using spectrophotometric methods [43].

2.2. Synthesis of eIF4G peptides

Peptides spanning residues 609–621 of human eIF4GI [44] (sequence: KKR**Y**DREF**LL**GFQ), referred to as *Hs* eIF4G peptide; residues 618–630 of *D. melanogaster* eIF4G [45] (sequence: KKQ**Y**DREQ**LL**QLR), referred to as *Dm* eIF4G peptide; and *Drosophila* eIF4G peptide with mutations Tyr621A, Leu626A and Leu627A (sequence: KKQADREQAAQLR), referred to as *Dm* eIF4G3A peptide, were synthesized by Metabion Company (Germany) using solid-phase peptide synthesis method with Fmoc-chemistry. The peptides were purified by RP-HPLC and quantised by MALDI-TOF: (*Hs* eIF4G peptide predicted mass: 1699,99 Da, measured mass: 1700,96 Da; *Dm* eIF4G peptide predicted mass: 1718 Da, measured mass: 1719.97 Da; *Dm* eIF4G3A peptide predicted mass: 1541.74 Da, measured mass: 1542.50 Da). Peptides were dissolved in 0.1% TFA in water and their concentrations in the case of *Hs* eIF4G and *Dm* eIF4G were also determined spectrophotometrically assuming $\varepsilon_{280} = 1490\ cm^{-1}\ M^{-1}$.

2.3. Cloning, mutagenesis, expression and purification of recombinant proteins

cDNAs of *Drosophila* eIF4Es were PCR-amplified and subcloned into pET30a expression vector (Novagen) in *Nde*I–*Bam*HI sites in the case of *Dm* eIF4E-1, *Dm* eIF4E-2, *Dm* eIF4E-4, and *Dm* 4EHP, and in *Nde*I–*Eco*RI sites in the case of *Dm* eIF4E-3, *Dm* eIF4E-5(12-232) and *Dm* eIF4E-7(9-429) without any affinity tag. Point mutations Cys217Ala and Cys228Ala in *Dm* eIF4E-4 were obtained using a PCR-based site-directed mutagenesis method.

For *Dm* eIF4E expression, constructs in pET30a were transformed into *Escherichia coli* BL21(DE3) or Rosetta 2(DE3) strains (Novagen). Bacteria were grown in LB medium to $OD_{600\ nm}$ of 1.0 and induced for 3 h at 37 °C by adding 0.5 mM isopropyl-1-thio-β-D-galactopyranoside (IPTG). Cells were harvested, resuspended in lysis buffer (20 mM HEPES/KOH (pH 7.5), 100 mM KCl, 1 mM EDTA, 2 mM DTT, 10% glycerol) and disrupted by sonication. After lysate centrifugation (30,000*g* for 30 min), supernatant was removed and the pellet was washed three or two times with wash buffer (20 mM HEPES/KOH (pH 7.2), 1 M guanidine hydrochloride, 2 mM DTT, 10% glycerol). Inclusion bodies were dissolved in 50 mM HEPES/KOH (pH 7.2), 6 M guanidine hydrochloride, 10% glycerol, and 2 mM DTT, and cell debris was removed by centrifugation (43,000*g* for 30 min). Proteins (diluted to a concentration lower than 0.1 mg/mL) were refolded using a one-step dialysis against 50 mM HEPES/KOH (pH 7.2), 100 mM KCl (or 50 mM KCl in the case of *Dm* eIF4E-3), 1.0 mM EDTA, and 2 mM DTT, and purified by ion exchange chromatography on a HiTrap SP column (GE Healthcare). Purified proteins were analysed on Bio-Safe Coomassie stained 15% acrylamide gel (in Suppl. Fig. S1) and their concentrations were determined based on absorption of protein samples using molar absorption coefficients as follows: $\varepsilon_{280} = 52{,}940\ M^{-1}\ cm^{-1}$ for *Dm* eIF4E-1; $\varepsilon_{280} = 52{,}940\ M^{-1}\ cm^{-1}$ for *Dm* eIF4E-2; $\varepsilon_{280} = 65{,}890\ M^{-1}\ cm^{-1}$ for *Dm* eIF4E-3; $\varepsilon_{280} = 51{,}450\ M^{-1}\ cm^{-1}$ for *Dm* eIF4E-4 and mutant *Dm* eIF4E-4_C217A/C228A; $\varepsilon_{280} = 55{,}920\ M^{-1}\ cm^{-1}$ for *Dm* eIF4E-5; $\varepsilon_{280} = 54{,}430\ M^{-1}\ cm^{-1}$ for *Dm* eIF4E-7; and $\varepsilon_{280} = 55{,}920\ M^{-1}\ cm^{-1}$ for *Dm* 4EHP, as calculated based on amino acid composition using an algorithm on ExPASy Server [46].

Human eIF4E protein was expressed in *E. coli* BL21(DE3) strain (Novagen) and purified from inclusion bodies as described above for *Drosophila* eIF4E proteins. Concentration of the purified protein was determined based on absorption of the protein sample using $\varepsilon_{280} = 52{,}940\ M^{-1}\ cm^{-1}$ calculated based on amino acid composition [46].

2.4. Protein structure homology modelling

Homologues of *D. melanogaster* eIF4E proteins were identified with PSI-Blast [47] searches (E-value threshold of 0.005) performed against

the NCBI nonredundant protein sequence database using sequences of *Dm* eIF4E-1, *Dm* eIF4E-2, *Dm* eIF4E-3, *Dm* eIF4E-4, *Dm* eIF4E-5, *Dm* eIF4E-7 and *Dm* 4EHP as queries. Multiple sequence alignment was derived using PCMA program [48] followed by some manual adjustments. Secondary structures were predicted with PSIPRED [49]. 3D models of *D. melanogaster* eIF4E proteins with cap analogues were constructed with MODELLER [50] using selected homologues of known structure as templates [51]. To obtain eIF4E isoforms bound to m^7GDP, *Dm* eIF4E-1/*Dm* eIF4E-2, *Dm* eIF4E-3, *Dm* eIF4E-4, *Dm* eIF4E-5, *Dm* eIF4E-7 were modelled based on *Dm* eIF4E-2 (PDB: 4AXG) [37] and human eIF4E (PDB: 2W97) [36], while *Dm* 4EHP was modelled based on human 4EHP (PDB: 2JGB) [52], *Pisum sativum* eIF4E (PDB: 2WMC) [53] and *Mus musculus* eIF4E (PDB: 1EJ1) [33]. 3D models of *Dm* eIF4E-4 and *Dm* eIF4E-5 in complex with eIF4G peptide were generated using the structure of *Dm* eIF4E-2 (PDB: 4UEC) [39]. Additionally, *Dm* eIF4E-1/*Dm* eIF4E-2, *Dm* eIF4E-3 and *Dm* eIF4E-5 were also modelled to obtain a 3D structure with m^7GpppA using *Dm* eIF4E-2 (PDB: 4AXG) and human eIF4E (PDB: 1IPB) [54] as templates.

2.5. Fluorescence binding assays

Fluorescence measurements leading to determination of association constants for eIF4E with cap analogues and peptides were performed as described previously [34,55]. Fluorescence titration curves were carried out on an LS-55 spectrofluorometer (Perkin Elmer Co., Norwalk, CT., USA), in 50 mM HEPES/KOH (pH 7.2), 0.5 mM EDTA and 1 mM DTT, adjusted with KCl to an ionic strength of 150 mM. The sample was thermostated at a temperature of 20.0 ± 0.3 °C and controlled with a thermocouple inside the cuvette. In the case of eIF4E–cap analogue titration, the protein fluorescence was excited at 280 nm or 290 nm and the fluorescence intensity was monitored at a single wavelength 340 nm or 345 nm. For titration of eIF4E with eIF4G peptides, the protein fluorescence was excited at 290 nm and observed at 345 nm, where the relative quenching of protein fluorescence upon peptide binding was the highest. Continuous titrations were performed by adding 1 μL aliquots of a cap analogue or peptide solution to 1400 μL of 0.1 μM solution of eIF4E alone or saturated with the peptide or cap analogue. The time for the integration of fluorescence signal upon each ligand addition was 30 s. The solution was mixed using magnetic stirring. Each titration consisted of 35–45 data points. Measured fluorescence intensities were corrected for dilution (<4%) and for the *inner filter* effect. Association equilibrium constants (K_{as}) were obtained by fitting a theoretical curve of corrected fluorescence intensity (F) upon total concentration of ligand ([L]) to the titration data according to the equation:

$$F = F(0) - [\mathrm{cx}] \cdot \left(\Delta\phi + \phi_{\mathrm{lig-free}}\right) + [\mathrm{L}] \cdot \phi_{\mathrm{lig-free}}$$

with the concentration of the cap analogue–eIF4E complex [cx] given by:

$$[\mathrm{cx}] = \frac{[\mathrm{L}] + [\mathrm{P_{act}}]}{2} + \frac{1 - \sqrt{(K_{as}([\mathrm{L}] - [\mathrm{P_{act}}]) + 1)^2 + 4K_{as} \cdot [\mathrm{P_{act}}]}}{2K_{as}}$$

where $\Delta\phi$ stands for the difference between the fluorescence efficiencies of the *apo* and ligand-bound protein; $\phi_{\mathrm{lig\text{-}free}}$ is the fluorescence efficiency of the free ligand; $F(0)$ is the initial fluorescence, and $[P_{act}]$ is the total concentration of the active protein [34]. The final K_{as} was calculated as a weighted average from three to ten independent titration series carried out for at least two independent preparations of the protein. Numerical least-squares nonlinear regression analysis was performed using ORGIN 6.0 from Microcal Software Inc., USA.

The Gibbs free energy of binding was calculated based on the K_{as} value according to the standard equation $\Delta G^o = -RT \ln K_{as}$.

3. Results and discussion

To compare the cap- and eIF4G-binding properties of *Drosophila* eIF4E family proteins, we applied the fluorescence titration, which is widely used to investigate the eIF4E–cap analogue association [34,55–58]. In this technique, quenching of the intrinsic fluorescence of conserved tryptophan residues in eIF4E (Fig. 1) due to binding of a cap analogue as well as eIF4G peptide is measured [34]. Next, we built homology models of *Dm* eIF4E structures and analysed the sequence and structure differences that may influence interaction with the cap and the eIF4G peptide in relation to the results obtained from binding studies.

3.1. The canonical eIF4E-1 from Drosophila binds cap analogues with significantly weaker affinity than its human counterpart

The measured K_{as} values for complexes of *Dm* eIF4E-1 and human eIF4E with different cap analogues are presented in Table 1. Similar to plant [58] and yeast eIF4Es [59], *Dm* eIF4E-1 bound all investigated cap analogues from 2.4- to 10-fold weaker than human eIF4E (Fig. 2A), keeping high specificity towards a methylated guanine at the N7 position and an extension of the phosphate chain (Table 2) [34,42]. For m^7GMP, the K_{as} is 0.82 ± 0.05 μM^{-1} for human eIF4E and 0.34 ± 0.01 μM^{-1} for *Dm* eIF4E-1, and for m^7GTP the K_{as} is 70.1 ± 1.2 μM^{-1} and 8.94 ± 0.27 μM^{-1} for human and *Drosophila* proteins, respectively.

Sequence comparison of human eIF4E and *Dm* eIF4E-1 showed that both proteins share all key residues that are required for cap binding (Fig. 1 and Table S1 for numbering). The main difference, which might affect cap binding affinity, seems to be an additional α-helix (amino acids 119–124) present in human eIF4E (Fig. 2B) and other vertebrates, but absent in *Drosophila*, yeast [60] and plant eIF4Es [61]. This region consists of large amino acids (KQQRRS) and lifts the position of the neighbouring β5β6 loop towards the cap binding pocket. As a consequence, in human eIF4E Lys159 located at the tip of β5β6 loop interacts tightly with the cap phosphate moiety, in contrast to its counterpart Lys201 in *Dm* eIF4E-1 (Fig. 2B). Crystal and NMR structures of mammalian eIF4E showed that the α- and β-phosphate groups of cap analogues are stabilised in the binding slot by a hydrogen bond formed with Arg157 and a salt bridge with Lys162 (numbering of human eIF4E) [34,35]. Additionally, binding studies with mutated mouse eIF4E showed that lysine 159 influences the binding of the γ-, δ- and ε-phosphate groups of cap to eIF4E [42]. Moreover, NMR studies of human eIF4E showed that closing of the β5β6 loop upon cap binding is important for interaction between the phosphate chain of the cap and the lateral chains of Arg157, Lys 159 and Lys162 [62]. Analysis of the changes in the standard Gibbs free energy of binding ($\Delta\Delta G^o$) (Table 2) revealed significant differences in binding of β-phosphate group of cap analogues by both eIF4E proteins. In the case of *Dm* eIF4E-1, the energy gain corresponding to addition of a β-phosphate group to m^7GMP is ca. 0.6 kcal/mol higher than for the human counterpart, whereas the differences in the energy changes $\Delta\Delta G^o$ between the proteins for binding of γ- and δ-phosphate groups are only 0.1 and 0.2 kcal/mol, respectively. The observed differences in the energy changes suggest weaker closing of *Dm* eIF4E-1 structure upon cap binding and weaker interaction of Lys201 with the phosphate chain of the cap, as compared to the human counterpart.

Besides N7 guanine methylation and presence of the phosphate moiety in the cap structure, which influence its binding to canonical vertebrate eIF4E factors, the third characteristic element of the cap structure is the influence of the second nucleoside, N (m^7GpppN). Addition of the second nucleoside to the mononucleotide in a cap analogue reduces significantly (ca. 10–12 fold) its ability to bind human eIF4E [34,42]. The same destabilisation effect caused by the presence of a second nucleoside was observed for *Dm* eIF4E-1. The K_{as} value for m^7GpppG is ca. 7-fold lower that the K_{as} observed for m^7GTP (Table 1).

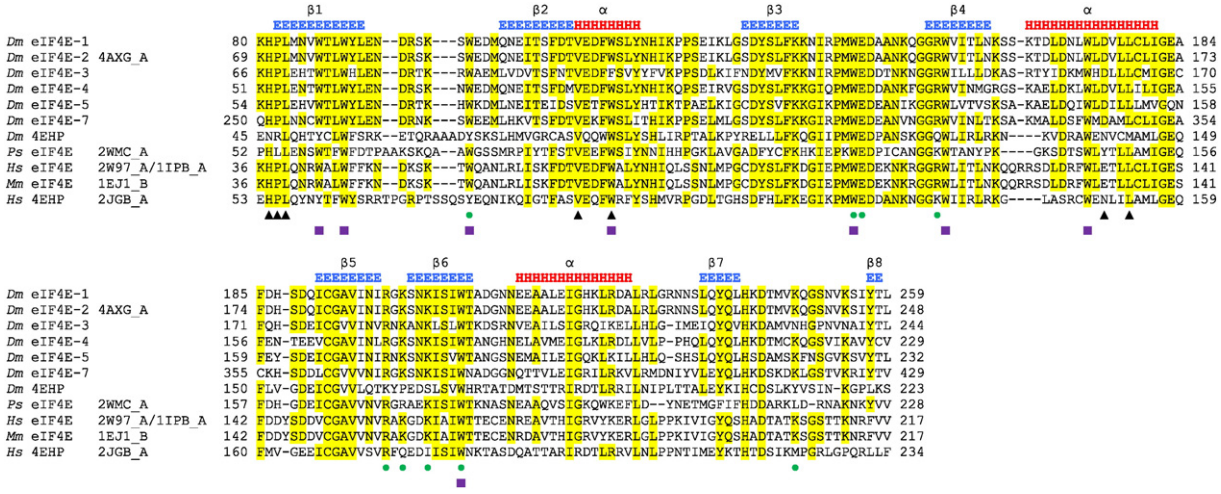

Fig. 1. Sequence comparison for eIF4E proteins. Multiple sequence alignment is shown for all *Drosophila melanogaster* eIF4E proteins and selected homologues of known structure (pea eIF4E, PDB: 2WMC; mouse eIF4E, PDB: 1EJ1; human eIF4E, PDB: 2W97/1IPB; human 4EHP, PDB: 2JGB). Conserved residues (50% or greater) are highlighted in yellow. Locations of secondary structure elements (E, β-strand; H, α-helix) in *Dm* eIF4E-2 (PDB: 4AXG) are marked above the sequences. Positions of amino acids in human/mouse eIF4E forming intermolecular contacts with cap [33,35] and eIF4G peptide [39,79] are indicated with green circles and black triangles, respectively. Positions of conserved eIF4E Trp residues are marked with violet squares.

3.2. Dm eIF4E-3 and Dm eIF4E-4 show the highest and lowest cap binding affinities, respectively, among Class I Dm eIF4Es

We next analysed the binding affinity of Class I *Drosophila* eIF4E proteins to different cap analogues. Despite the presence of conserved key residues responsible for cap recognition (Fig. 1, Table S1), *Drosophila* proteins bound cap analogues with diverse affinities (Fig. 3A). The K_{as} values for complexes of *Drosophila* eIF4E isoforms with a series of various cap analogues are presented in Table 1, and the corresponding standard Gibbs free energies of binding (ΔG^{o}) are shown in Table S2.

Among the seven analysed *Dm* eIF4E proteins, the highest cap binding affinities are found for *Dm* eIF4E-3, with K_{as} values higher or comparable to those obtained for the human eIF4E, with the exception of m^7GTP, m^7Gp4 and m^7GppppG, which are bound with higher affinity by the human eIF4E. *Dm* eIF4E-3 binds m^7GTP ca. 3.5-fold weaker than human eIF4E, but 2-fold stronger than *Dm* eIF4E-1 and ca. 9-fold stronger than *Dm* eIF4E-4, which among all *Dm* eIF4E proteins shows the lowest ability to bind cap analogues. A characteristic feature of *Dm* eIF4E-3 is its high specificity towards dinucleotide cap analogues (Tables 1 and 2). Previous studies showed that in vertebrate eIF4E proteins [34,56,57], addition of a second guanosine to m^7GTP and m^7Gp4 gives a disadvantageous entropic effect of about +1.4 kcal/mol and +1.8 kcal/mol calculated as the change in the Gibbs free energy of binding ($\Delta\Delta G^{o}$). The observed K_{as} values for m^7GpppG in complex with vertebrate eIF4E were even 2.5–3.0-fold lower than those observed for eIF4E- complexes with m^7GDP [34,56,57]. Addition of further three nucleotides to the cap structure (m^7GpppNpNpNpN) restored the K_{as} values to the level observed for m^7GTP [63]. These results show that the second nucleoside of the cap is not well stabilised within the cap binding slot itself and, additionally, its presence destabilises intermolecular contacts between the second, third and fourth phosphate groups of dinucleotide cap analogues and positively charged amino acids located at the entrance to the cap binding slot. Moreover, the short α-helix following the β7 strand does not exist in human eIF4E complexes with dinucleotide cap analogues, as compared to complexes with mononucleotide cap analogues [35,36]. The presence of the long loop β7β8 may make the structure of eIF4E in complex with a dinucleotide cap analogue more open as compared to that with a mononucleotide (Fig. 3B and C). For *Dm* eIF4E-3, the destabilising effect on complex formation resulting from the addition of the second guanosine to m^7Gppp is only +0.5 kcal/mol, whereas m^7GppppG and m^7Gp4 are bound with similar K_{as} values of $35.7 \pm 1.1\ \mu M^{-1}$ and $38.4 \pm 2.0\ \mu M^{-1}$, respectively. For the other Class I *Dm* eIF4E proteins, complex destabilisation resulting from the presence of the second nucleoside was observed. The energetic cost of adding a guanosine moiety to m^7GTP is ca. +1.0 kcal/mol (Table 2), similar to what is observed for the human eIF4E. Strong binding of the cap α-phosphate group by *Dm* eIF4E-3, with very low binding to the β-, γ- and δ-phosphate moieties, can explain the high specificity of this isoform towards dinucleotide cap analogues. The K_{as} value for complex of *Dm* eIF4E-3 with m^7GMP is 3.6-

Table 1
Equilibrium association constants (K_{as}) for the complexes of *Drosophila* and human eIF4E proteins from Class I and Class II with a series of various cap analogues.

Cap analogue	Class I							Class II	
	Hs eIF4E	*Dm* eIF4E-1	*Dm* eIF4E-2	*Dm* eIF4E-3	*Dm* eIF4E-4	*Dm* eIF4E-5	*Dm* eIF4E-7	*Hs* 4EHP*	*Dm* 4EHP
	K_{as} (μM^{-1})								
m^7GMP	0.82 ± 0.05	0.34 ± 0.01	0.30 ± 0.02	2.96 ± 0.06	0.10 ± 0.01	0.83 ± 0.03	0.44 ± 0.01	0.07 ± 0.01	0.35 ± 0.01
m^7GDP	18.24 ± 0.24	2.70 ± 0.05	2.58 ± 0.03	11.94 ± 0.19	0.66 ± 0.02	7.13 ± 0.10	1.72 ± 0.02	0.23 ± 0.03	0.94 ± 0.03
m^7GTP	70.1 ± 1.2	8.94 ± 0.27	8.47 ± 0.28	19.29 ± 0.52	2.16 ± 0.07	17.9 ± 1.4	5.3 ± 0.1	0.70 ± 0.04	2.89 ± 0.12
m^7Gp_4	320 ± 18	29.9 ± 0.9	28.4 ± 1.6	38.4 ± 2.0	7.55 ± 0.25	106.3 ± 2.6	30.2 ± 0.8	1.20 ± 0.04	4.4 ± 0.3
m^7GpppG	6.25 ± 0.07	1.29 ± 0.04	1.23 ± 0.04	8.24 ± 0.28	0.38 ± 0.01	4.44 ± 0.20	1.56 ± 0.01	0.17 ± 0.01	0.84 ± 0.03
$m^{7,2'\text{-}O}_2$GpppG	5.95 ± 0.13	1.27 ± 0.01	1.04 ± 0.03	8.96 ± 0.56	0.35 ± 0.01	5.46 ± 0.10	1.17 ± 0.01	0.12 ± 0.01	0.89 ± 0.01
m^7GpppA	3.08 ± 0.03	0.78 ± 0.07	0.73 ± 0.03	5.88 ± 0.10	0.24 ± 0.01	3.16 ± 0.09	0.64 ± 0.03	0.13 ± 0.01	0.71 ± 0.01
m^7GpppC	3.45 ± 0.18	0.98 ± 0.02	0.94 ± 0.01	4.79 ± 0.35	0.26 ± 0.01	2.46 ± 0.08	0.92 ± 0.03	0.16 ± 0.02	0.73 ± 0.04
m^7GppppG	49.9 ± 1.2	7.03 ± 0.10	6.61 ± 0.15	35.7 ± 1.1	1.73 ± 0.03	22.5 ± 3.0	5.5 ± 0.2	0.72 ± 0.02	2.49 ± 0.17
GTP	0.044 ± 0.002	0.036 ± 0.005	0.05 ± 0.01	0.034 ± 0.001	0.07 ± 0.01	0.056 ± 0.003	0.07 ± 0.01	0.031 ± 0.002	0.014 ± 0.002

* data from [56].

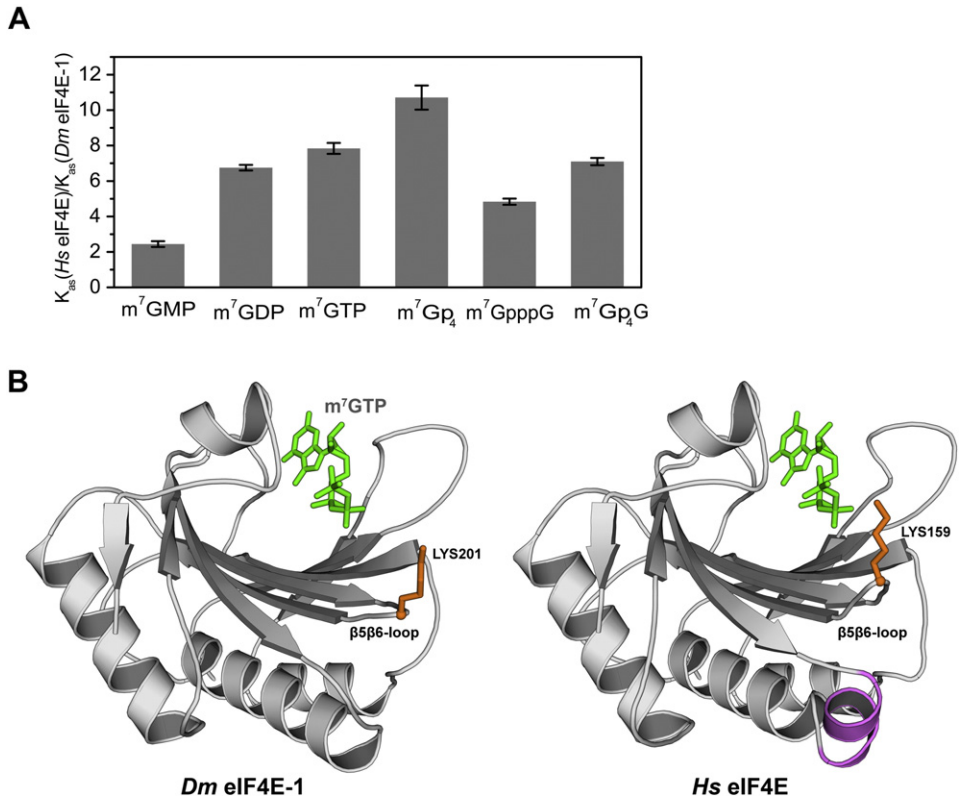

Fig. 2. Cap binding ability of *Drosophila* eIF4E-1 protein and human eIF4E. (A) Comparison of binding affinities of *Dm* eIF4E-1 and human eIF4E protein to various cap analogues on the basis of the ratio of K_{as} values as determined from fluorescence titration measurements in the same conditions. (B) Comparison of a 3D model for *Dm* eIF4E-1 and crystal structure of human eIF4E (PDB: 2W97). Additional short α-helix in human eIF4E is shown in violet, while side chains of the conserved lysine located on β5β6 loop, which is closer to the cap binding slot in human protein, are shown in orange. Cap analogue (m^7GTP) is shown in green.

fold higher than that for the human eIF4E ($K_{as} = 2.96 \pm 0.06\ \mu M^{-1}$ and $0.82 \pm 0.05\ \mu M^{-1}$, respectively). The energetic gain resulting from the extension of m^7GMP to m^7GDP is about −0.8 kcal/mol for *Dm* eIF4E-3, whereas for the human protein it is about −1.81 kcal/mol. Upon addition of the third and fourth phosphate groups to cap analogues, the energetic gain for *Dm* eIF4E-3 is about −0.3 kcal/mol and −0.4 kcal/mol, whereas for the human eIF4E it is about −0.8 kcal/mol and −0.9 kcal/mol, respectively (Table 2). Consequently, the second nucleotide of the cap does not disturb the interaction between the cap phosphate chain and positively charged amino acids in *Dm* eIF4E-3, in contrast to other eIF4Es, which bind β- γ- and δ-phosphate groups strongly. Additionally, according to our model, His234 in *Dm* eIF4E-3, located in the β7β8 loop (Fig. 3B), is likely to cause the observed high affinity of *Dm* eIF4E-3 for dinucleotide cap analogues. This aromatic amino acid probably takes part in the stacking interactions with the second base of the cap and is replaced by Ser207, Gln249, Gln238, Gln219 and Leu419 in human eIF4E, *Dm* eIF4E-1, *Dm* eIF4E-2, *Dm* eIF4E-4 and *Dm* eIF4E-7, respectively (Fig. 1 and Fig. 3B). Prediction of stacking interactions between His234 of *Dm* eIF4E-3 and the second base of the cap is also confirmed by weaker binding to dinucleotide cap analogues containing pyrimidines instead of purines (Table 1). *Dm* eIF4E-5 has an aromatic residue, Phe222, at the position corresponding to His234 in *Dm* eIF4E-3. The K_{as} values for complexes of *Dm* eIF4E-5 with dinucleotide cap analogues (m^7GpppN) are ca. 3-fold higher than those observed for *Dm* eIF4E-1 and comparable to those of the human eIF4E. However, the energetic cost resulting from the addition of a second nucleoside to m^7Gppp is about +1.0 kcal/mol, 2-fold higher than that observed for *Dm* eIF4E-3. *Dm* eIF4E-5 shows stronger binding to the β-, γ- and δ-phosphate groups of mononucleotide cap analogues (Table 2), and probably opening of the eIF4E structure after dinucleotide

Table 2
Changes in standard Gibbs free energy (ΔΔG^o), showing the contribution of structural elements of the 5′ mRNA cap to binding free energy of eIF4E–cap complexes. ΔΔG^o values were calculated as the difference in the binding free energy (ΔG^o) of eIF4E to cap analogues, which varies in single structural modifications.

Structural changes	Class I							Class II	
	Hs eIF4E	*Dm* eIF4E-1	*Dm* eIF4E-2	*Dm* eIF4E-3	*Dm* eIF4E-4	*Dm* eIF4E-5	*Dm* eIF4E-7	*Hs* 4EHP	*Dm* 4EHP
	ΔΔG^o (kcal/mol)								
Methylation of the guanosine ring in N^7 position ΔΔG^o = ΔG^o (m^7Gp_n) − ΔG^o (Gp_n)									
GTP → m^7GTP	−4.29 ± 0.03	−3.20 ± 0.09	−2.98 ± 0.12	−3.69 ± 0.03	−2.02 ± 0.04	−3.36 ± 0.05	−2.49 ± 0.04	−1.80 ± 0.05	−3.07 ± 0.09
Successive addition of the phosphate groups ΔΔG^o = ΔG^o (m^7Gp_{n+1}) − ΔG^o (m^7Gp_n)									
m^7GMP- > m^7GDP	−1.81 ± 0.03	−1.21 ± 0.03	−1.25 ± 0.04	−0.81 ± 0.02	−1.08 ± 0.06	−1.24 ± 0.02	−0.80 ± 0.02	−0.71 ± 0.15	−0.58 ± 0.02
m^7GDP- > m^7GTP	−0.78 ± 0.02	−0.70 ± 0.02	−0.69 ± 0.02	−0.28 ± 0.02	−0.69 ± 0.03	−0.54 ± 0.05	−0.65 ± 0.01	−0.64 ± 0.09	−0.66 ± 0.03
m^7GTP- > m^7Gp_4	−0.88 ± 0.04	−0.70 ± 0.02	−0.70 ± 0.04	−0.40 ± 0.03	−0.73 ± 0.03	−1.04 ± 0.05	−1.02 ± 0.02	−0.31 ± 0.03	−0.25 ± 0.05
Addition of the second nucleoside ΔΔG^o = ΔG^o (m^7Gp_nG) − ΔG^o (m^7Gp_n)									
m^7GTP- > m^7Gp_3G	1.41 ± 0.02	1.13 ± 0.03	1.13 ± 0.03	0.50 ± 0.03	1.01 ± 0.02	0.981 ± 0.05	0.71 ± 0.01	0.82 ± 0.04	0.72 ± 0.03
m^7Gp_4- > m^7Gp_4G	1.08 ± 0.04	0.84 ± 0.02	0.85 ± 0.03	0.04 ± 0.03	0.86 ± 0.02	0.90 ± 0.08	0.99 ± 0.03	0.29 ± 0.02	0.34 ± 0.06

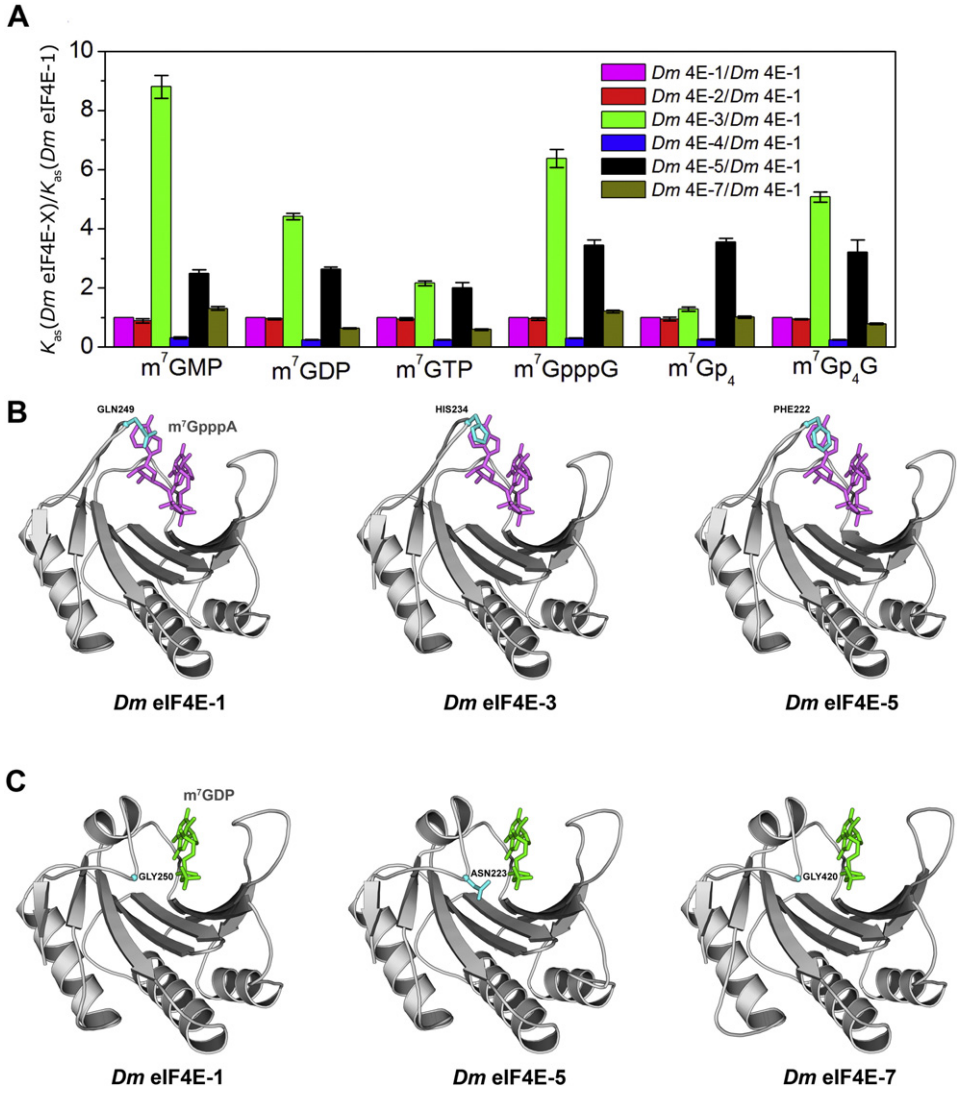

Fig. 3. Differences in the cap binding ability of Class I *Drosophila* eIF4Es. (A) Comparison of the binding affinities of *Dm* eIF4Es to various cap analogues determined from fluorescence titration measurements in the same conditions. Values are given as the K_{as} ratio of the given isoform over that of *Dm* eIF4E-1. (B) Possible stabilisation of the second base of the cap by stacking interactions with His243 in *Dm* eIF4E-3 and Phe222 in *Dm* eIF4E-5. Cap analogue (m^7GpppA) is shown in violet. (C) Additional potential stabilisation of the phosphate group of cap by interaction with Asn223 in *Dm* eIF4E-5. Cap analogue (m^7GDP) is shown in green.

cap analogue binding is not compensated by stacking interactions between the second base of the cap and Phe222.

Dm eIF4E-5 shows the highest affinities for dinucleotide cap analogues with methyl at the 2′-hydroxyl group of the ribose moiety of m^7Guo. The K_{as} value for $m_2^{7,2\text{-}O}$GpppG is 1.4 fold higher than for m^7GpppG. For the other *Dm* eIF4E isoforms and the human eIF4E, the positive influence of ribose methylation in C2′ position on cap-binding was not observed (Table 1). The structures of mammalian eIF4Es show that the ribose hydroxyl group of m^7Guo is located outside the protein surface and does not interact directly with eIF4E [33, 35].

eIF4E-7 is the *Drosophila* isoform with the highest molecular weight and the longest N-terminal region (31–249), which seems to be unstructured, as indicated by our sequence and structure analysis. We observed that eIF4E-7 binds cap analogues with affinities comparable to those of *Dm* eIF4E-1. Similarly, *Dm* eIF4E-2, obtained via alternative splicing of the product of the gene encoding *Dm* eIF4E-1, showed binding affinity for cap analogues similar to that of *Dm* eIF4E-1 (Fig. 3A). These two isoforms differ only in the N-terminal region, as the core and the C-terminal region are identical.

The lowest cap-binding affinity among the *Dm* eIF4E isoforms was observed for *Dm* eIF4E-4, despite the conservation of all key residues involved in cap binding (Fig. 1). This isoform shows a similar decrease of K_{as} values for all investigated monomethylated cap analogues, as compared to K_{as} observed for *Dm* eIF4E-1 (Table 1). *Dm* eIF4E-4 binds to monomethylated cap analogues 3.2- to 4.1-fold weaker than *Dm* eIF4E-1. The energetic effects corresponding to the extension of the cap phosphate chain and to the addition of the second nucleoside are similar for both proteins (Table 2). The main difference observed for the *Dm* eIF4E-4 isoform was its lower specificity to N7 guanosine methylation. The energetic gain observed upon GTP methylation was only -2.02 ± 0.04 kcal/mol, whereas for *Dm* eIF4E-1 it was -3.20 ± 0.09 kcal/mol and for *Dm* eIF4E-3 -3.69 ± 0.03 kcal/mol (Table 2). For this isoform, we observed the tendency for dimerisation (in Suppl. Fig. S2 A); it is likely that two cysteines in *Dm* eIF4E-4 (Cys217 and Cys228) are responsible for this effect. The cysteines are located in the β7β8 loop and the last strand β8, which may form cross disulphide bonds. Replacement of these cysteines by alanine residues abrogates the protein dimerisation (in Suppl. Fig. S2 A) but does not affect its cap and eIF4G binding affinities (in Suppl. Fig. S2B).

3.3. Different contribution of cap's phosphate groups on stabilization of Dm Class I eIF4E–cap complexes

The interactions between the phosphate moiety of the cap and the side chains of basic residues located at the entrance to the eIF4E cap binding slot play a critical role in eIF4E–cap complex formation. These interactions are mediated by networks of salt bridges and hydrogen bonds [33,35]. The extension of the phosphate chain of mono- and dinucleotide cap analogues results in an increase of vertebrate eIF4E binding affinities [34,42,56,57]. In mammalian eIF4Es, the strongest influence on cap binding is exerted by the cap α- and β-phosphate groups that interact with the side chains of Arg112, Arg157, and Lys162 (numbering of human eIF4E). The total energy of α-phosphate and β-phosphate stabilisation is ca. −3.0 kcal/mol and ca. −1.8 kcal/mol, respectively (Table 2) [34,35]. The extension of the phosphate chain by the γ- and δ-moieties gives an energetic gain of −0.8 kcal/mol and −0.9 kcal/mol, respectively, similar to what has been described for hydrogen bond formation [64] (Table 2). For all *Dm* eIF4E isoforms, an increase of K_{as} values as a result of the phosphate chain extension was also observed. However, the stabilising effect of individual phosphate groups on binding with proteins was very diverse (Tables 1 and 2).

Dm eIF4E-3 recognizes the α-phosphate group with the highest affinity, with K_{as} value for m^7GMP about 9-fold higher than *Dm* eIF4E-1 and about 3.6-fold higher than human eIF4E and *Dm* eIF4E-5. Addition of the β-phosphate (m^7GMP → m^7GDP) causes a significant increase of the binding affinity in the case of *Dm* eIF4E-1, *Dm* eIF4E-2, *Dm* eIF4E-4, and *Dm* eIF4E-5. K_{as} values for the respective complexes with m^7GDP are from 6.6 to 8.6-fold higher than with m^7GMP. However, the observed increase in cap binding affinity for these proteins is two-fold lower, as compared to the human protein. The energetic gain of introducing the β-phosphate group into the cap is about −1.2 kcal/mol, which suggests that these isoforms can form one or two hydrogen bonds/salt bridges with the β-phosphate moiety. These results are in contrast to what we observed for *Dm* eIF4E-3 and *Dm* eIF4E-7, with a $\Delta\Delta G^o$ of −0.8 kcal/mol, corresponding to the creation of only one hydrogen bond/salt bridge. The changes in the binding energy accompanying the cap phosphate chain extension in mononucleotide analogues (m^7GDP → m^7GTP → m^7Gp_4) is ca. −0.70 kcal/mol for *Dm* eIF4E-1, *Dm* eIF4E-2 and *Dm* eIF4E-4, implying that these proteins probably form one hydrogen bond with the cap γ- and δ-phosphate groups, similar to what has been reported for mammalian eIF4Es (Table 2) [34,42]. In the case of *Dm* eIF4E-3, the corresponding $\Delta\Delta G^o$ value associated with the addition of γ- and δ-phosphate groups to the cap is ca. −0.28 kcal/mol and −0.4 kcal/mol, respectively, which is weaker than the typical values reported for the hydrogen bond in a solvent-accessible region within proteins [64]. The reason of this might be a partial dispersion of the positive charged in the cap binding pocket.

In contrast to other *Dm* eIF4E isoforms and human eIF4E, a significant increase in cap binding affinity associated with the addition of an extra δ-phosphate group was observed for *Dm* eIF4E-5 and *Dm* eIF4E-7. They bind m^7Gp_4 about 6-fold stronger than m^7GTP, while other *Drosophila* isoforms bind m^7Gp_4 up to 3.5-fold stronger than m^7GTP. In addition, *Dm* eIF4E-5 binds m^7Gp_4 2.5-fold stronger than other isoforms. The main difference between *Dm* eIF4E-5 and the other isoforms, responsible for a higher affinity to m^7Gp_4 might be Asn223, which may interact with the δ-phosphate group (Fig. 3C). This residue is replaced by Gly in *Dm* eIF4E-1, -2, -3, -4 and -7. Based on our modelling, we see no significant changes in *Dm* eIF4E-7 that might be responsible for its higher affinity to the m^7Gp_4 cap analogue.

3.4. Drosophila 4EHP shows a low cap binding affinity but still higher than its human counterpart

Dm 4EHP belongs to the Class II of eIF4E family proteins [6]. Members of this class have either Tyr or Phe in the position corresponding to Trp43 and Tyr instead of Trp56 of human eIF4E [6]. As a consequence, in *Dm* 4EHP and human 4EHP the N7-methylguanine moiety of the cap is sandwiched between tyrosine and tryptophan residues (Tyr68 and Trp114 in *Dm* 4EHP and Tyr78 and Trp124 in human 4EHP [52]) (Fig. 4). In contrast, in Class I eIF4E proteins, the N7-methylguanine is stacked between two tryptophan residues (Trp56 and Trp102 in the human protein). The lack of the ability to interact with eIF4G renders both, *Drosophila* and human 4EHP, translation repressors [26,30]. Through binding with both, the cap and diverse 4E-BPs that directly or indirectly bind to 3′-UTR elements, 4EHP inhibits translation of specific mRNAs [14,15,30,31]. Recent fluorescence binding studies showed that human 4EHP recognises cap analogues very weakly, with K_{as} for m^7GTP 100-fold lower than that of the human eIF4E [56]. This difference in cap affinity probably prevents uncontrolled competition between 4EHP and eIF4E for cap binding in vivo.

We compared the binding affinities of *Dm* 4EHP for different cap analogues. As reported for human 4EHP, also for *Dm* 4EHP we observed lower binding affinity for cap analogues as compared to *Dm* eIF4E-1, but the differences in ability to bind the cap are not as high as it was observed for human proteins (Table 1). *Dm* 4EHP binds m^7GTP with a K_{as} value of 2.89 ± 0.12 μM^{-1}, which is 3.1-fold lower than the value observed for *Dm* eIF4E-1 and similar to the *Dm* eIF4E-4 value. Thus, *Dm* 4EHP affinity for m^7GTP is 4-fold higher than the K_{as} value reported for its human counterpart under the same conditions [56].

Since *Dm* 4EHP specificity towards N7-methylguanine of cap is similar to that of *Dm* eIF4E-1 (Table 2), analyses of our data suggest that the weak affinity of *Dm* 4EHP for the cap might not be caused by the Trp to Tyr substitution in the stacking interaction with m^7G. We observed that the corresponding energetic gain upon addition of a methyl group at the guanine moiety of GTP is −3.07 ± 0.09 kcal/mol and −3.20 ± 0.09 kcal/mol for *Dm* 4EHP and *Dm* eIF4E-1, respectively. In addition, substitution of Trp56 by tyrosine residue in human eIF4E did not reduce its binding affinity [56]. Both, our sequence analysis and 3D structure modelling, suggest that the most prominent difference that might explain the weak cap binding ability of *Dm* 4EHP seems to be the lack of conserved Arg and Lys residues (Arg156, Lys201 and Lys204 in *Dm* eIF4E-1), which may interact with the phosphate groups of the cap. In *Dm* 4EHP, they are replaced by glutamine (Gln124), proline (Pro166) and serine (Ser169), respectively (Fig. 4). Lack of arginine and lysine residues in these positions can be partially compensated in *Dm* 4EHP by Arg128. This residue is substituted by an uncharged amino acid in the other *Drosophila* eIF4E isoforms (e.g. Thr160 in *Dm* eIF4E-1).

The binding studies of *Drosophila* and human 4EHP revealed some differences and similarities in their abilities to bind the cap. First of all, human 4EHP shows a very low specificity to N7 guanosine methylation, what distinguishes it from *Dm* 4EHP. The changes in binding energy corresponding to methylation of the guanine moiety in GTP is only −1.80 ± 0.05 kcal/mol for human 4EHP, whereas for *Dm* 4EHP it is −3.07 ± 0.09 kcal/mol. These differences might be associated with the extension of the β1β2 loop by five amino acids in human 4EHP, as compared to eIF4E, which may increase the loop's flexibility. In *Dm* 4EHP, this loop is extended only by three amino acids (Figs. 1 and 4). As a consequence, the aromatic ring of Tyr78 in human 4EHP might adopt a slightly different alignment and may overlap with the N7-methylguanine moiety. Again, both proteins are lacking the full network of interactions created between the conserved Arg and Lys residues and the phosphate groups of the cap that are present in canonical eIF4Es. In both proteins, Lys159, Lys162 (numbering of human eIF4E) and in *Dm* 4EHP also Arg112 are substituted by non-positively charged amino acids (Fig. 4). However, in human 4EHP, the α-phosphate group is stabilised by an extra hydrogen bond with $N^{\varepsilon 2}$ of His110 [52], which is replaced by Tyr100 in *Dm* 4EHP and by glycine residue in both, *Dm* eIF4E-1 and human eIF4E. What is more, the γ-phosphate group is stabilized by water-mediated hydrogen bond with the additional Arg138 in human and Arg128 in *Drosophila* 4EHP (Fig. 4). The differences in intermolecular contacts between phosphate chain of cap and

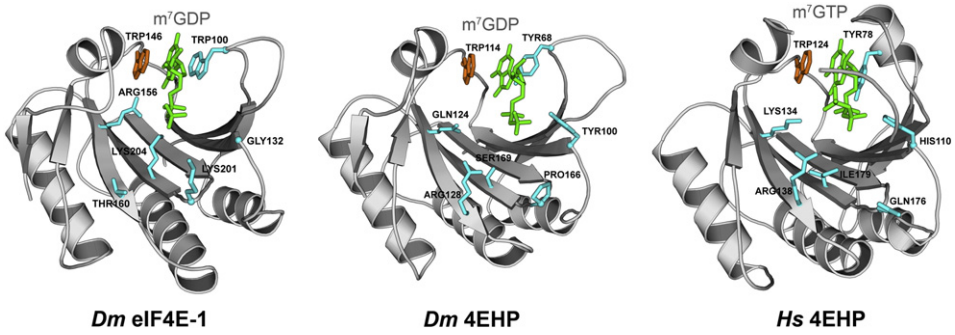

Fig. 4. Comparison of Class I and Class II eIF4E structures in complex with cap analogues. *Dm* eIF4E-1 (Class I) and *Dm* 4EHP (Class II) modelled structures were compared with reported structure of human 4EHP (Class II, PDB: 2JGB). Amino acids critical for differences in binding affinity for cap analogues are indicated in cyan. Conserved tryptophan is shown in orange. Cap analogues are depicted in green.

amino acids observed between both 4EHP proteins did not transfer to differences in the Gibbs free energy of phosphate group binding between proteins. The sequential additions of the next three phosphate groups to m^7GMP gave the same energetic gain ($\Delta\Delta G^o$) for both proteins (Table 2). These results suggest that the difference in cap binding abilities between *Drosophila* and human 4EHP proteins concerns the binding of N7-methylguanosine.

3.5. Cooperativity between binding of the eIF4G peptide and cap analogues is observed only for Dm eIF4E-4 isoforms

It has been shown by both coimmunoprecipitation experiments and the yeast two-hybrid systems that all *Drosophila* Class I eIF4E proteins bind *Dm* eIF4G, in contrast to both *Drosophila* and mammalian 4EHP [7,26,28,65,66]. Moreover, recent studies [38,39] have shown that *Dm* eIF4E-2 binds *Dm* eIF4G only via the canonical 4E-binding motif 621YDREQLL627 in eIF4EG. In six Class I *Drosophila* eIF4E proteins, all residues involved in eIF4G binding by the C-motif are conserved (Fig. 1), whereas in *Dm* eIF4E-3 and *Dm* 4EHP they are not [26].

Several biophysical and biological studies have shown that the association of eIF4G to eIF4E in the *apo* form enhances cap binding by eIF4E. This cooperativity effect has been observed in the case of both, human and yeast, eIF4Es, where interaction with eIF4G increased cap affinity 2-fold [67] and up to 100-fold, respectively [68]. It has been suggested that this effect is important for formation of an active eIF4F complex and therefore for translation control [69]. In disagreement with these observations, other biophysical studies have shown that binding of a 90-residue-long fragment of eIF4G to mammalian eIF4E did not increase the cap binding affinity of eIF4E [34,70].

Next, we wanted to extend our fluorescence-based comparative analyses of cap binding to *Drosophila* eIF4E proteins in complex with a peptide (13 amino acids) consisting of the eIF4E-binding site of either human or *Drosophila* eIF4G. As a control, we used a *Drosophila* eIF4G peptide, in which the residues important for eIF4E binding, Tyr621, Leu626 and Leu627, are substituted by Ala.

First, we determined the K_{as} values for binary complexes of *Dm* eIF4E with *Dm* eIF4G peptide, taking advantage of the fact that binding to eIF4E dorsal surface leads to quenching of the intrinsic eIF4E fluorescence through interaction with a tryptophan residue corresponding to human Trp73. The obtained K_{as} values for *Drosophila* (except for *Dm* eIF4E-3, which does not have a Trp residue in this position) and human eIF4Es are presented in Table 3. We observed K_{as} of the order of 10^6 M^{-1}, which is similar to the values published for mammalian proteins with short eIF4G peptides containing only the C-motif [34,67,71,72]. As expected, *Dm* 4EHP did not interact with *Dm* eIF4G peptide [65]. We also observed no interaction between the peptide *Dm* eIF4G3A and any of all *Dm* eIF4E isoforms. Unexpectedly, we observed the strongest binding affinity between *Dm* eIF4G peptide and *Dm* eIF4E-4, with K_{as} value for the binary complex ca. 7-fold higher than that for the corresponding complex with *Dm* eIF4E-1 (Table 3). We also observed formation of a strong complex in the case of *Dm* eIF4E-5 isoform with K_{as} value ca. 3.5-fold higher than for *Dm* eIF4E-1 and *Dm* eIF4E-2. The most crucial difference that might explain higher affinity of *Dm* eIF4E-4 and *Dm* eIF4E-5 to eIF4G peptides corresponds to the replacement of *Dm* eIF4E-2 Met73 by Glu55 and Glu58 in *Dm* eIF4E-4 and *Dm* eIF4E-5, respectively (Fig. 5C). These glutamic acids may form additional interactions with two conserved lysines, namely Lys618 and Lys619 in *Dm* eIF4G, and Lys609 and Lys610 in human eIF4G. Interestingly, both, *Dm* eIF4E-4 and human eIF4E, showed the highest affinity for their own eIF4G peptide, even though the peptides differ from each other only in 5 amino acids. The differences in binding affinities between human eIF4G and *Dm* eIF4G to the corresponding eIF4Es are by 2-fold (Table 3). These results suggest that the composition of amino acids in the C-binding motif and in the neighbouring regions, especially the presence of arginine and lysine

Table 3
Equilibrium association constants (K_{as}) of the binary complexes of the *Drosophila* and human eIF4E protein from Class I with the *Drosophila* and human eIF4G peptides that contain the respective eIF4E-binding site, with the non-binding counterpart in the case of the *Drosophila* eIF4G peptide, and for the ternary complexes: peptide–eIF4E–m^7GTP of previously peptide-saturated eIF4E.

	Class I							Class II
	Hs eIF4E	*Dm* eIF4E-1	*Dm* eIF4E-2	*Dm* eIF4E-3[a]	*Dm* eIF4E-4	*Dm* eIF4E-5	*Dm* eIF4E-7	*Dm* 4EHP
	K_{as} [μM^{-1}] for peptide							
Dm eIF4G peptide	4.44 ± 0.62	0.99 ± 0.21	1.16 ± 0.08	ND	7.39 ± 0.60	3.44 ± 0.78	1.15 ± 0.52	<0.07
Dm eIF4G3A peptide	<0.17	No binding	<0.03	ND	<0.03	No binding	<0.08	No binding
Hs eIF4G peptide	7.08 ± 0.30	0.74 ± 0.23	1.29 ± 0.06	ND	4.64 ± 0.14	2.33 ± 0.33	ND	ND
	K_{as} [μM^{-1}] for m^7GTP when eIF4E is peptide-saturated							
Apo	73.5 ± 2.4	8.09 ± 0.25	7.34 ± 0.12	21.97 ± 0.72	2.12 ± 0.06	19.7 ± 0.8	5.70 ± 0.13	2.76 ± 0.10
Dm eIF4G peptide saturated	70.3 ± 3.1	7.71 ± 0.20	6.06 ± 0.08	20.86 ± 0.76	3.70 ± 0.05	17.3 ± 3.0	5.52 ± 0.07	2.71 ± 0.08
Dm eIF4G3A peptide saturated	73.4 ± 3.2	8.30 ± 0.45	7.04 ± 0.09	20.2 ± 2.4	2.24 ± 0.08	18.0 ± 0.7	5.56 ± 0.07	2.96 ± 0.05
Hs eIF4G peptide saturated	68.4 ± 5.5	6.77 ± 0.15	7.00 ± 0.67	ND	4.00 ± 0.06	21.4 ± 0.8	ND	ND

[a] Substitution of Trp residue taking a part in binding of eIF4G and others 4E-BP proteins by Phe residue.

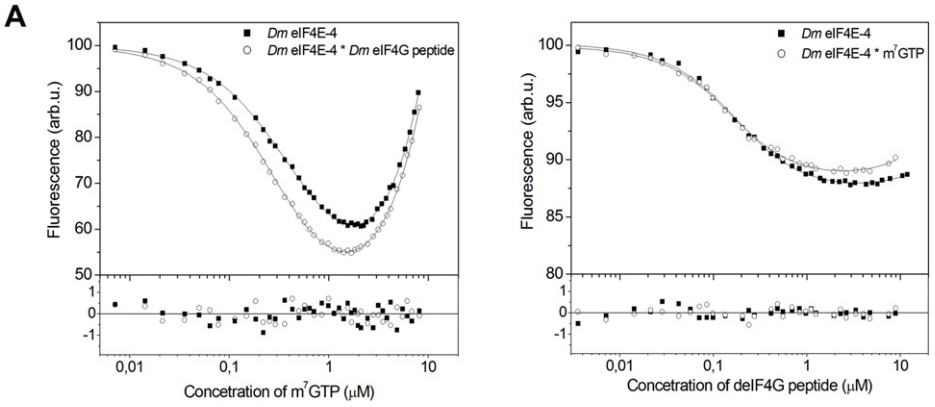

B

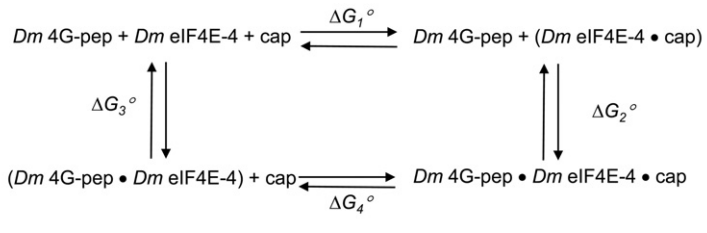

$$\Delta\Delta G = \Delta G_2^\circ - \Delta G_1^\circ = \Delta G_4^\circ - \Delta G_3^\circ$$

Formation of ternary complex	ΔG_1° (kcal/mol)	ΔG_2° (kcal/mol)	$\Delta\Delta G^\circ$ (kcal/mol)	ΔG_3° (kcal/mol)	ΔG_4° (kcal/mol)	$\Delta\Delta G^\circ$ (kcal/mol)
Dm eIF4G-pep + *Dm* eIF4E-4 + m^{7}GTP	-8.48±0.02	-8.81±0.01	**-0.32±0.02**	-9.21±0.05	-9.44±0.05	**-0.23±0.07**
Dm eIF4G-pep + *Dm* eIF4E-4 + m^{7}GpppG	-7.51±0.02	-7.73±0.01	**-0.21±0.03**	-9.21±0.05	-9.51±0.04	**-0.30±0.06**

C

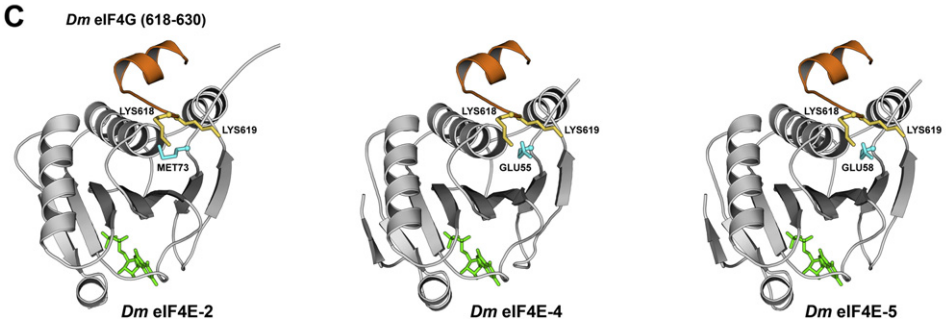

Fig. 5. Cooperativity in the formation of the ternary complex eIF4G–*Dm* eIF4E-4–cap analogue. (A) Comparison of the fluorescence titration curves for the formation of *Dm* eIF4E-4 binary and ternary complexes with m^{7}GTP and the *Dm* eIF4G-peptide. (B) Thermodynamic cycle for ternary complex formation of *Dm* eIF4G-peptide, *Dm* eIF4E-4 and either m^{7}GTP or m^{7}GpppG cap analogues with the changes in the standard free energy ($\Delta\Delta G^o$) as calculated from free energy of binding (ΔG^o) determined for sequential binding of each member of the complex. (C) Comparison of the reported structure of *Dm* eIF4E-2 (PDB: 4UEC) and the modelled structures of *Dm* eIF4E-4 and *Dm* eIF4E-5 in complex with the *Dm* eIF4G peptide and cap analogue. *Dm* eIF4G peptide and cap analogue are indicated in orange and green, respectively. Critical *Dm* eIF4G lysines are shown in yellow. Amino acids critical for the difference in the binding affinity for *Dm* eIF4G are depicted in cyan.

residues (KKX**YXR/KX$_2$L**ϕX$_2$R/K), play an important role in diversification of eIF4G and other 4E-BPs binding affinities among eIF4Es, as also suggested Peter and co-workers [39].

Then, we asked whether eIF4G binding to *Drosophila* eIF4E proteins exerts a cooperative effect on their ability to bind cap analogues. To address this question, we determined K_{as} values for m^{7}GTP binding, when the eIF4G peptide was already bound to *Dm* eIF4Es. The saturation concentration of eIF4G peptide for each eIF4E isoform was calculated based on the equation for concentration of eIF4E–eIF4G peptide complex using the determined K_{as} values. A short (13 amino acids) eIF4G peptide enhanced binding to m^{7}GTP only in the case of *Dm* eIF4E-4, by 2-fold (Table 3). To probe the synergy in formation of the ternary complex of eIF4G peptide–eIF4E-4–cap analogues, we conducted fluorescence binding titration for all four binding reactions involving *Dm* eIF4G peptides, *Dm* eIF4E-4 and one of two cap analogues, namely, m^{7}GTP and m^{7}GpppG (Fig. 5A). The obtained results are summarised in Fig. 5A, B and in Suppl. Table S3. In the case of *Dm* eIF4E-4, we observed a cooperative activity in ternary complexes formation. Both, eIF4G peptides and cap analogues, increased *Dm* eIF4E-4 affinity for the other ligand by an average of 0.2–0.3 kcal/mol in the case of *Dm* eIF4G peptide and 0.3–0.4 kcal/mol in the case of human eIF4G (1.5–2.0-fold increase of K_{as} values). Equivalent experiments for human complexes did not show the cooperativity in formation of ternary complex (in Suppl. Table S3). Previous studies on human complex formation showed both eIF4E cap-affinity enhancement by eIF4G binding [67], as well as lack of influence of eIF4G on eIF4E cap binding [34,70]. However, the eIF4E–eIF4G binding studies for human protein were performed with different length of eIF4GI and eIF4GII fragments (short 12–20 amino acid peptides and 90-residue-long eIF4G fragment), and according to our and previous studies the length and sequences composition of eIF4G peptide

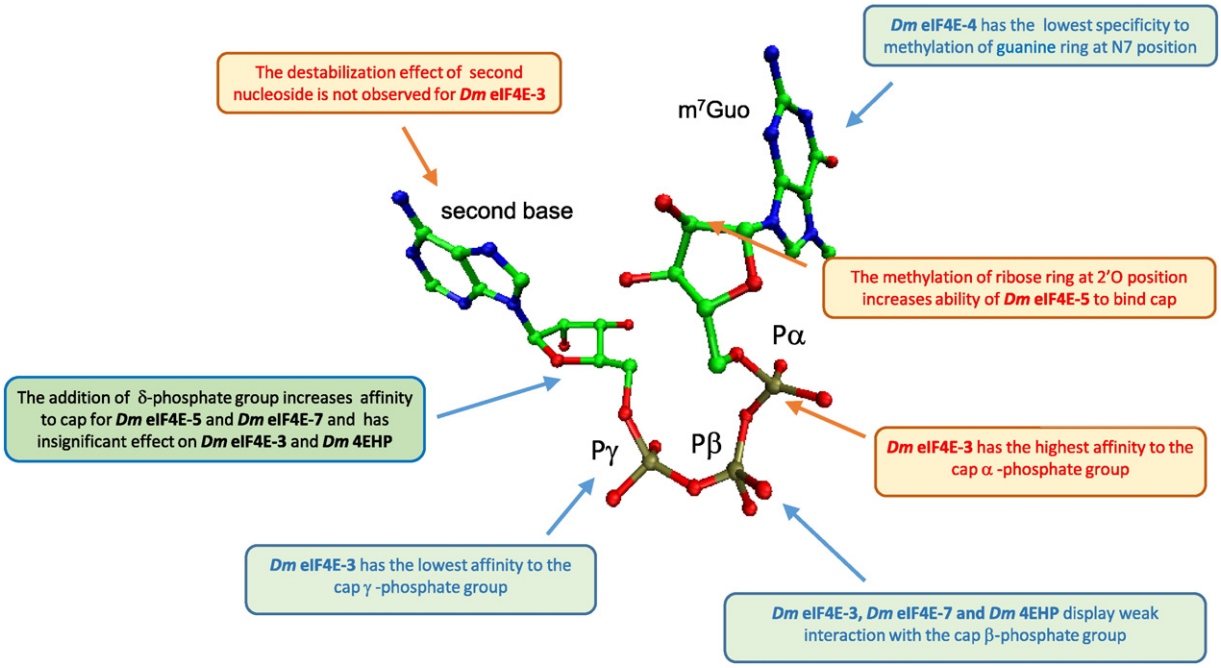

Fig. 6. Schematic representation of the cap structure and its interactions with *Dm* eIF4Es. The differences in ability of the *Drosophila* eIF4E proteins to bind the individual elements of a 5′ mRNA cap structure are indicated. The cap is represented by m^7GpppA. For consistency with text, the numbering of phosphate groups applied for mononucleotide cap analogues was used.

is important for the interaction with eIF4E [39,71,72]. Furthermore, in contrast to *Drosophila* eIF4E, the human protein probably contains a second NC-motif for eIF4G binding [72,73].

Although the cooperativity in formation of ternary eIF4G peptide–eIF4E–cap analogue complexes remains controversial, some NMR, MS and crystallographic studies have shown significant structural differences between a binary and a ternary complex [36,62,74]. eIF4E binding to the cap results in structural rearrangements, not only around the region of cap binding, but also on the dorsal surface of eIF4E and, conversely, eIF4G binding alters the conformation around the cap binding slot especially in the region that interacts with phosphate moiety of the cap [62].

4. Conclusion

Using fluorescence binding studies combined with sequence/structure analyses, we demonstrate shared and distinct features of cap binding by *Drosophila* eIF4E family members. Although Class I *Dm* eIF4Es have all the key conserved residues involved in cap recognition, differences in amino acid sequences confer different binding affinities to the elements of the cap structure: N7-methylguanosine, phosphate chain and the second nucleoside (Fig. 6). The K_{as} values for complexes of *Dm* eIF4Es with individual cap analogues differed by as much as 14-fold. However, the N7-methyl group is crucial for cap recognition by all *Dm* eIF4E proteins.

According to our 3D models, *Dm* eIF4E-3 and eIF4E-5 display, typical for nuclear cap binding complex (CBC), stabilisation of the second cap nucleoside by potential stacking interaction with an aromatic residue: His234 and Phe222, respectively. In human CBC, the second nucleoside is stabilised by stacking interaction with Tyr138 [75] and its substitution by alanine reduces CBC binding affinity for m^7GpppG about 4-fold [76,77]. *Dm* eIF4E-3 binds dinucleotide cap analogues 1.3–1.9 fold stronger than human eIF4E. Interestingly, *Dm* eIF4E-3 expression is restricted to testes of adult male flies and regulates translation during spermatogenesis by forming specific eIF4F complexes with eIF4G and eIF4G2, and its activity is not regulated by 4E-BP. Moreover, male flies lacking eIF4E-3 are viable but are completely sterile [28].

Other *Drosophila* eIF4E cognate, for which the biological role is known, is 4EHP that acts as a translation repressor by competing with eIF4E for binding of the mRNA cap. It represses translation of specific maternal mRNAs, such as *caudal* (*cad*) and *hunchback* (*hb*), which are important for establishing the correct anterior-posterior axis polarity in the *Drosophila* embryo [30,31]. 4EHP inhibits translation of *cad* mRNA by simultaneous binding with the cap and Bicoid, which in turn binds to 3′UTR of *cad* mRNA. In the case of *hb* mRNA, 4EHP binds the cap and a Brat protein member of NRE complex required for inhibition of *hb* mRNA [31,78]. In mammals, such inhibition of mechanism involving 4EHP was documented during maturation of mouse oocyte, where 4EHP in complex with Prep1 protein inhibits translation of *Hox4* mRNA [14]. Interactions of 4EHP with specific protein partners together with the lack of eIF4G binding, as well as its low affinity for the cap in *apo* form were considered key factors for translational inhibition of specific mRNAs. The significantly lower (100–200 fold) cap binding affinity of human 4EHP as compared to human eIF4E [56] can prevent cap recognition of all mRNA and hence uncontrolled translation inhibition. *Drosophila* 4EHP binds only 3-fold weaker to m^7GTP and m^7GpppG than *Dm* eIF4E-1, suggesting the existence of different additional control mechanisms of 4EHP availability for mRNA recognition in *Drosophila* and human.

Altogether, our studies showed that some local sequence differences play an important role in the eIF4E–cap interactions that might have an impact on their biological role.

Transparency document

The Transparency document associated with this article can be found, in online version.

Acknowledgement

We are grateful to Janusz Stepinski and Jacek Jemielity from Division of Biophysics and Centre of New Technology at University of Warsaw for providing us with cap analogues and to Kamil Steczkiewicz for help in preparation of the figures. This research was supported by the Polish

National Science Centre, [UMO-2012/07/B/NZ1/00118 to Edward Darzynkiewicz and JZ, UMO-2011/02/A/NZ2/00014 and UMO-2014/15/B/NZ1/03357 to KG], and by the European Social Fund [EU, UDA-POKL.04.01.01-00-072/09-00 to KK]. We thank the Biopolymers Laboratory, Division of Biophysics, Institute of Experimental Physics, Faculty of Physics, University of Warsaw, for use the Thermocycler PCR "CXF-96" and Autoclave "Laboklav 135V" co-financed by the European Union within the European Regional Development Fund Project [POIG.02.01.00-14-122/09].

Appendix A. Supplementary data

Supplementary data to this article can be found online at http://dx.doi.org/10.1016/j.bbapap.2016.06.015.

References

[1] N. Sonenberg, A.G. Hinnebusch, Regulation of translation initiation in eukaryotes: mechanisms and biological targets, Cell 136 (2009) 731–745, http://dx.doi.org/10.1016/j.cell.2009.01.042.
[2] R.J. Jackson, C.U.T. Hellen, T.V. Pestova, The mechanism of eukaryotic translation initiation and principles of its regulation, Nat. Rev. Mol. Cell Biol. 11 (2010) 113–127, http://dx.doi.org/10.1038/nrm2838.
[3] J.D. Richter, N. Sonenberg, Regulation of cap-dependent translation by eIF4E inhibitory proteins, Nature 433 (2005) 477–480, http://dx.doi.org/10.1038/nature03205.
[4] G. Hernández, M. Altmann, P. Lasko, Origins and evolution of the mechanisms regulating translation initiation in eukaryotes, Trends Biochem. Sci. 35 (2010) 63–73, http://dx.doi.org/10.1016/j.tibs.2009.10.009.
[5] G. Hernández, P. Vazquez-Pianzola, Functional diversity of the eukaryotic translation initiation factors belonging to eIF4 families, Mech. Dev. 122 (2005) 865–876, http://dx.doi.org/10.1016/j.mod.2005.04.002.
[6] B. Joshi, K. Lee, D.L. Maeder, R. Jagus, Phylogenetic analysis of eIF4E-family members, BMC Evol. Biol. 5 (2005) 48, http://dx.doi.org/10.1186/1471-2148-5-48.
[7] B. Joshi, A. Cameron, R. Jagus, Characterization of mammalian eIF4E-family members, Eur. J. Biochem. 271 (2004) 2189–2203, http://dx.doi.org/10.1111/j.1432-1033.2004.04149.x.
[8] R.E. Rhoads, eIF4E: new family members, new binding partners, new roles, J. Biol. Chem. 284 (2009) 16711–16715, http://dx.doi.org/10.1074/jbc.R900002200.
[9] A.V. Evsikov, C.M. de Evsikova, Evolutionary origin and phylogenetic analysis of the novel oocyte-specific eukaryotic translation initiation factor 4E in Tetrapoda, Dev. Genes Evol. 219 (2009) 111–118, http://dx.doi.org/10.1007/s00427–008–0268-2.
[10] R.M. Patrick, K.S. Browning, The eIF4F and eIFiso4F complexes of plants: an evolutionary perspective, Comp. Funct. Genomics 2012 (2012) 287814, http://dx.doi.org/10.1155/2012/287814.
[11] R. Jagus, T.R. Bachvaroff, B. Joshi, A.R. Place, Diversity of eukaryotic translational initiation factor eIF4E in protists, Comp. Funct. Genomics 2012 (2012) 134839, http://dx.doi.org/10.1155/2012/134839.
[12] G.D. Jones, E.P. Williams, A.R. Place, R. Jagus, T.R. Bachvaroff, The alveolate translation initiation factor 4E family reveals a custom toolkit for translational control in core dinoflagellates, BMC Evol. Biol. 15 (2015) 14, http://dx.doi.org/10.1186/s12862-015-0301-9.
[13] B.D. Keiper, B.J. Lamphear, A.M. Deshpande, M. Jankowska-Anyszka, E.J. Aamodt, T. Blumenthal, et al., Functional characterization of five eIF4E isoforms in *Caenorhabditis elegans*, J. Biol. Chem. 275 (2000) 10590–10596, http://dx.doi.org/10.1074/jbc.275.14.10590.
[14] J.C. Villaescusa, C. Buratti, D. Penkov, L. Mathiasen, J. Planagumà, E. Ferretti, et al., Cytoplasmic Prep1 interacts with 4EHP inhibiting Hoxb4 translation, PLoS One 4 (2009), e5213http://dx.doi.org/10.1371/journal.pone.0005213.
[15] M. Morita, L.W. Ler, M.R. Fabian, N. Siddiqui, M. Mullin, V.C. Henderson, et al., A novel 4EHP-GIGYF2 translational repressor complex is essential for mammalian development, Mol. Cell. Biol. 32 (2012) 3585–3593, http://dx.doi.org/10.1128/MCB.00455-12.
[16] J. Uniacke, C.E. Holterman, G. Lachance, A. Franovic, M.D. Jacob, M.R. Fabian, et al., An oxygen-regulated switch in the protein synthesis machinery, Nature 486 (2012) 126–129, http://dx.doi.org/10.1038/nature11055.
[17] J. Uniacke, J.K. Perera, G. Lachance, C.B. Francisco, S. Lee, Cancer cells exploit eIF4E2-directed synthesis of hypoxia response proteins to drive tumor progression, Cancer Res. 74 (2014) 1379–1389, http://dx.doi.org/10.1158/0008-5472.CAN-13-2278.
[18] S. Timpano, J. Uniacke, Human cells cultured under physiological oxygen utilize two cap-binding proteins to recruit distinct mRNAs for translation, J. Biol. Chem. (2016)http://dx.doi.org/10.1074/jbc.M116.717363 jbc.M116.717363.
[19] M.J. Osborne, L. Volpon, J.a. Kornblatt, B. Culjkovic-Kraljacic, A. Baguet, K.L.B. Borden, eIF4E3 acts as a tumor suppressor by utilizing an atypical mode of methyl-7-guanosine cap recognition. Proc. Natl. Acad. Sci. U. S. A. 110 (2013) 3877–3882, http://dx.doi.org/10.1073/pnas.1216862110.
[20] N. Minshall, M.H. Reiter, D. Weil, N. Standart, CPEB interacts with an ovary-specific eIF4E and 4E-T in early Xenopus oocytes, J. Biol. Chem. 282 (2007) 37389–37401, http://dx.doi.org/10.1074/jbc.M704629200.
[21] M. Jankowska-Anyszka, B.J. Lamphear, E.J. Aamodt, T. Harrington, E. Darzynkiewicz, R. Stolarski, R.E. Roads, Multiple isoforms of eukaryotic protein-synthesis initiation-factor-4E in *Caenorhabditis elegans* can distinguish between monomethylated and trimethylated messenger RNA cap structur, J. Biol. Chem. 273 (1998) 10538–10542, http://dx.doi.org/10.1074/jbc.273.17.10538.
[22] R.S. Mangio, S. Votra, D. Pruyne, The canonical eIF4E isoform of *C. elegans* regulates growth, embryogenesis, and germline sex-determination. Biology Open. (2015) 1–9, http://dx.doi.org/10.1242/bio.011585.
[23] M.A. Henderson, E. Cronland, S. Dunkelbarger, V. Contreras, S. Strome, B.D. Keiper, A germline-specific isoform of eIF4E (IFE-1) is required for efficient translation of stored mRNAs and maturation of both oocytes and sperm, J. Cell Sci. 122 (2009) 1529–1539, http://dx.doi.org/10.1242/jcs.046771.
[24] I. Kawasaki, M.H. Jeong, Y.H. Shim, Regulation of sperm-specific proteins by IFE-1, a germline-specific homolog of eIF4E, in *C. elegans*, Mol. Cells 31 (2011) 191–197, http://dx.doi.org/10.1007/s10059–011-0021-y.
[25] T.D. Dinkova, B.D. Keiper, L. Nadejda, E.J. Aamodt, R.E. Rhoads, N.L. Korneeva, Translation of a small subset of *Caenorhabditis elegans* mRNAs is dependent on a specific eukaryotic translation initiation factor 4E isoform translation of a small subset of *Caenorhabditis elegans* mRNAs is dependent on a specific eukaryotic translation in, Mol. Cell. Biol. 25 (2005) 100–113, http://dx.doi.org/10.1128/MCB.25.1.100.
[26] G. Hernández, M. Altmann, J.M. Sierra, H. Urlaub, R. Diez Del Corral, P. Schwartz, et al., Functional analysis of seven genes encoding eight translation initiation factor 4E (eIF4E) isoforms in *Drosophila*, Mech. Dev. 122 (2005) 529–543, http://dx.doi.org/10.1016/j.mod.2004.11.011.
[27] G. Tettweiler, M. Kowanda, P. Lasko, N. Sonenberg, G. Hernández, The distribution of eIF4E-family members across Insecta, Comp. Funct. Genomics 2012 (2012) 960420, http://dx.doi.org/10.1155/2012/960420.
[28] G. Hernandez, H. Han, V. Gandin, L. Fabian, T. Ferreira, J. Zuberek, et al., Eukaryotic initiation factor 4E-3 is essential for meiotic chromosome segregation, cytokinesis and male fertility in *Drosophila*, Development 139 (2012) 3211–3220, http://dx.doi.org/10.1242/dev.073122.
[29] S. Ghosh, P. Lasko, Loss-of-function analysis reveals distinct requirements of the translation initiation factors eIF4E, eIF4E-3, eIF4G and eIF4G2 in *Drosophila* spermatogenesis, PLoS One 10 (2015), e0122519http://dx.doi.org/10.1371/journal.pone.0122519.
[30] P.F. Cho, F. Poulin, Y.A. Cho-Park, I.B. Cho-Park, J.D. Chicoine, P. Lasko, et al., A new paradigm for translational control: inhibition via 5′-3′ mRNA tethering by bicoid and the eIF4E cognate 4EHP, Cell 121 (2005) 411–423, http://dx.doi.org/10.1016/j.cell.2005.02.024.
[31] P.F. Cho, C. Gamberi, Y.A. Cho-Park, I.B. Cho-Park, P. Lasko, N. Sonenberg, Cap-dependent translational inhibition establishes two opposing morphogen gradients in *Drosophila* embryos, Curr. Biol. 16 (2006) 2035–2041, http://dx.doi.org/10.1016/j.cub.2006.08.093.
[32] A. Yarunin, R.E. Harris, M.P. Ashe, H.L. Ashe, Patterning of the *Drosophila* oocyte by a sequential translation repression program involving the d4EHP and Belle translational repressors, RNA Biol. 8 (2011) 904–912, http://dx.doi.org/10.4161/rna.8.5.16325.
[33] J. Marcotrigiano, A. Gingras, N. Sonenberg, S.K. Burley, Cocrystal structure of the messenger RNA 5′ cap-binding protein (eIF4E) bound to 7-methyl-GDP, Cell 89 (1997) 951–961.
[34] A. Niedzwiecka, J. Marcotrigiano, J. Stepinski, M. Jankowska-Anyszka, A. Wyslouch-Cieszynska, M. Dadlez, et al., Biophysical studies of eIF4E cap-binding protein: recognition of mRNA 5′ cap structure and synthetic fragments of eIF4G and 4E-BP1 proteins, J. Mol. Biol. 319 (2002) 615–635, http://dx.doi.org/10.1016/S0022-2836(02)00328-5.
[35] K. Tomoo, X. Shen, K. Okabe, Y. Nozoe, S. Fukuhara, S. Morino, et al., Structural features of human initiation factor 4E, studied by X-ray crystal analyses and molecular dynamics simulations, J. Mol. Biol. 328 (2003) 365–383, http://dx.doi.org/10.1016/S0022-2836(03)00314-0.
[36] C.J. Brown, C.S. Verma, M.D. Walkinshaw, D.P. Lane, Crystallization of eIF4E Complexed With eIF4GI Peptide and Glycerol Reveals Distinct Structural Differences Around the Cap-binding Site, 2009 1905–1911.
[37] K. Kinkelin, K. Veith, M. Grunwald, F. Bono, Crystal structure of a minimal eIF4E-Cup complex reveals a general mechanism of eIF4E regulation in translational repression, RNA 18 (2012) 1624–1634, http://dx.doi.org/10.1261/rna.033639.112.
[38] C. Igreja, D. Peter, C. Weiler, E. Izaurralde, 4E-BPs require non-canonical 4E-binding motifs and a lateral surface of eIF4E to repress translation, Nat. Commun. 5 (2014) 4790, http://dx.doi.org/10.1038/ncomms5790.
[39] D. Peter, C. Igreja, R. Weber, L. Wohlbold, C. Weiler, L. Ebertsch, et al., Molecular architecture of 4E-BP translational inhibitors bound to eIF4E, Mol. Cell 1–14 (2015)http://dx.doi.org/10.1016/j.molcel.2015.01.017.
[40] E. Darzynkiewicz, I. Ekiel, S.M. Tahara, L.S. Seliger, A.J. Shatkin, Chemical synthesis and characterization of 7-methylguanosine cap analogues, Biochemistry 24 (1985) 1701–1707, http://dx.doi.org/10.1021/bi00328a020.
[41] J. Jemielity, T. Fowler, J. Zuberek, J. Stepinski, M. Lewdorowicz, A. Niedzwiecka, et al., Novel "anti-reverse" cap analogs with superior translational properties. RNA (New York, N.Y.) 9 (2003) 1108–1122, http://dx.doi.org/10.1261/rna.5430403.
[42] J. Zuberek, J. Jemielity, A. Jablonowska, J. Stepinski, M. Dadlez, R. Stolarski, et al., Influence of electric charge variation at residues 209 and 159 on the interaction of eIF4E with the mRNA 5′ terminus, Biochemistry 43 (2004) 5370–5379, http://dx.doi.org/10.1021/bi030266t.
[43] A. Cai, M. Jankowska-Anyszka, A. Centers, L. Chlebicka, J. Stepinski, R. Stolarski, et al., Quantitative assessment of mRNA cap analogues as inhibitors of in vitro translation, Biochemistry 38 (1999) 8538–8547, http://dx.doi.org/10.1021/bi9830213.
[44] T. Ota, Y. Suzuki, T. Nishikawa, T. Otsuki, T. Sugiyama, R. Irie, et al., Complete sequencing and characterization of 21,243 full-length human cDNAs, Nat. Genet. 36 (2004) 40–45, http://dx.doi.org/10.1038/ng1285.
[45] G. Hernández, M. del Mar Castellano, M. Agudo, J.M. Sierra, Isolation and characterization of the cDNA and the gene for eukaryotic translation initiation factor 4G from

Drosophila melanogaster, Eur. J. Biochem. / FEBS. 253 (1998) 27–35 (http://www.ncbi.nlm.nih.gov/pubmed/9578457).
[46] C.N. Pace, F. Vajdos, L. Fee, G. Grimsley, T. Gray, How to measure and predict the molar absorption coefficient of a protein. Protein Sci. 4 (1995) 2411–2423, http://dx.doi.org/10.1002/pro.5560041120.
[47] S. Altschul, T. Madden, A. Schaffer, J. Zhang, Z. Zhang, W. Miller, et al., Gapped BLAST and PSI- BLAST: a new generation of protein database search programs, Nucleic Acids Res. 25 (1997) 3389–3402http://nar.oxfordjournals.org/content/25/17/3389.short.
[48] J. Pei, R. Sadreyev, N.V. Grishin, PCMA: fast and accurate multiple sequence alignment based on profile consistency, Bioinformatics 19 (2003) 427–428, http://dx.doi.org/10.1093/bioinformatics/btg008.
[49] L.J. McGuffin, K. Bryson, D.T. Jones, The PSIPRED protein structure prediction server. Bioinformat. (Oxford, England). 16 (2000) 404–405, http://dx.doi.org/10.1093/bioinformatics/16.4.404.
[50] A. Fiser, A. Šali, MODELLER: generation and refinement of homology-based protein structure models, Methods Enzymol. 374 (2003) 461–491, http://dx.doi.org/10.1016/S0076-6879(03)74020-8.
[51] K. Ginalski, L. Rychlewski, Protein structure prediction of CASP5 comparative modelling and fold recognition targets using consensus alignment approach and 3D assessment, proteins: structure, Funct. Genet. 53 (2003) 410–417, http://dx.doi.org/10.1002/prot.10548.
[52] P. Rosettani, S. Knapp, M.-G. Vismara, L. Rusconi, A.D. Cameron, Structures of the human eIF4E homologous protein, h4EHP, in its m7GTP-bound and unliganded forms, J. Mol. Biol. 368 (2007) 691–705, http://dx.doi.org/10.1016/j.jmb.2007.02.019.
[53] J.A. Ashby, C.E.M. Stevenson, G.E. Jarvis, D.M. Lawson, A.J. Maule, Structure-based mutational analysis of eIF4E in relation to sbm1 resistance to Pea seed-borne mosaic virus in Pea, PLoS One 6 (2011), e15973http://dx.doi.org/10.1371/journal.pone.0015873.
[54] K. Tomoo, X. Shen, K. Okabe, Y. Nozoe, S. Fukuhara, S. Morino, et al., Crystal structures of 7-methylguanosine 5′-triphosphate (m(7)GTP)- and P(1)-7-methylguanosine-P(3)-adenosine-5′,5′-triphosphate (m(7)GpppA)-bound human full-length eukaryotic initiation factor 4E: biological importance of the C-terminal flexible region, Biochem. J. 362 (2002) 539–544, http://dx.doi.org/10.1042/0264-6021:3620539.
[55] A. Niedzwiecka, J. Stepinski, J.M. Antosiewicz, E. Darzynkiewicz, R. Stolarski, Biophysical Approach to Studies of Cap-eIF4E Interaction by Synthetic Cap Analogs, Elsevier Inc., First Edit, 2007http://dx.doi.org/10.1016/S0076-6879(07)30009-8.
[56] J. Zuberek, D. Kubacka, A. Jablonowska, J. Jemielity, J. Stepinski, N. Sonenberg, et al., Weak binding affinity of human 4EHP for mRNA cap analogs. RNA (New York, N.Y.) 13 (2007) 691–697, http://dx.doi.org/10.1261/rna.453107.
[57] D. Kubacka, R.N. Miguel, N. Minshall, E. Darzynkiewicz, N. Standart, J. Zuberek, Distinct features of Cap binding by eIF4E1b proteins, J. Mol. Biol. 427 (2015) 387–405, http://dx.doi.org/10.1016/j.jmb.2014.11.009.
[58] A. Kropiwnicka, K. Kuchta, M. Lukaszewicz, J. Kowalska, J. Jemielity, K. Ginalski, et al., Five eIF4E isoforms from *Arabidopsis thaliana* are characterized by distinct features of cap analogs binding, Biochem. Biophys. Res. Commun. 456 (2015) 47–52, http://dx.doi.org/10.1016/j.bbrc.2014.11.032.
[59] K. Kiraga-Motoszko, A. Niedzwiecka, A. Modrak-Wojcik, J. Stepinski, E. Darzynkiewicz, R. Stolarski, Thermodynamics of molecular recognition of mRNA 5 cap by yeast eukaryotic initiation factor 4E, J. Phys. Chem. B 115 (2011) 8746–8754, http://dx.doi.org/10.1021/jp2012039.
[60] J.D. Gross, N.J. Moerke, T. Von Der Haar, A.a. Lugovskoy, A.B. Sachs, J.E.G. McCarthy, et al., Ribosome loading onto the mRNA cap is driven by conformational coupling between eIF4G and eIF4E, Cell. 115 (2003) 739–750, http://dx.doi.org/10.1016/S0092–8674(03)00975–9.
[61] A.F. Monzingo, S. Dhaliwal, A. Dutt-Chaudhuri, A. Lyon, J.H. Sadow, D.W. Hoffman, et al., The structure of eukaryotic translation initiation factor-4E from wheat reveals a novel disulfide bond, Plant Physiol. 143 (2007) 1504–1518, http://dx.doi.org/10.1104/pp.106.093146.
[62] L. Volpon, M.J. Osborne, I. Topisirovic, N. Siddiqui, K.L.B. Borden, Cap-free structure of eIF4E suggests a basis for conformational regulation by its ligands, EMBO J. 25 (2006) 5138–5149, http://dx.doi.org/10.1038/sj.emboj.7601380.
[63] Y. Yoffe, J. Zuberek, M. Lewdorowicz, Z. Zeira, C. Keasar, I. Orr-Dahan, et al., Cap-binding activity of an eIF4E homolog from Leishmania, RNA (New York, N.Y.) 10 (2004) 1764–1775, http://dx.doi.org/10.1261/rna.7520404.
[64] B.A. Shirley, P. Stanssens, U. Hahn, C.N. Pace, Contribution of hydrogen bonding to the conformational stability of ribonuclease T1, Biochemistry 31 (1992) 725–732, http://dx.doi.org/10.1021/bi00118a013.
[65] E. Rom, H.C. Kim, a.C. Gingras, J. Marcotrigiano, D. Favre, H. Olsen, et al., Cloning and characterization of 4EHP, a novel mammalian eIF4E-related cap-binding protein, J. Biol. Chem. 273 (1998) 13104–13109.
[66] A.R. Tee, J.a. Tee, J. Blenis, Characterizing the interaction of the mammalian eIF4E-related protein 4EHP with 4E-BP1, FEBS Lett. 564 (2004) 58–62, http://dx.doi.org/10.1016/S0014–5793(04)00313–8.
[67] D.E. Friedland, W.N.B. Wooten, J.E. Lavoy, C.H. Hagedorn, D.J. Goss, A mutant of eukaryotic protein synthesis initiation factor eIF4E, Biochemistry 44 (2005) 4546–4550.
[68] M. Ptushkina, T. Von Der Haar, M.M. Karim, J.M.X. Hughes, J.E.G. McCarthy, Repressor binding to a dorsal regulatory site traps human eIF4E in a high cap-affinity state, EMBO J. 18 (1999) 4068–4075, http://dx.doi.org/10.1093/emboj/18.14.4068.
[69] W.C. Merrick, eIF4F: a retrospective, J. Biol. Chem. 290 (2015) 24091–24099, http://dx.doi.org/10.1074/jbc.R115.675280.
[70] S.V. Slepenkov, N.L. Korneeva, R.E. Rhoads, Kinetic mechanism for assembly of the m7GpppG · eIF4E · eIF4G complex, J. Biol. Chem. 283 (2008) 25227–25237, http://dx.doi.org/10.1074/jbc.M801786200.
[71] C.J. Brown, J.J. Lim, T. Leonard, H.C.a. Lim, C.S.B. Chia, C.S. Verma, et al., Stabilizing the eIF4G1 α-helix increases its binding affinity with eIF4E: implications for peptidomimetic design strategies, J. Mol. Biol. 405 (2011) 736–753, http://dx.doi.org/10.1016/j.jmb.2010.10.045.
[72] Y. Umenaga, K.S. Paku, Y. In, T. Ishida, K. Tomoo, Identification and function of the second eIF4E-binding region in N-terminal domain of eIF4G: comparison with eIF4E-binding protein, Biochem. Biophys. Res. Commun. 414 (2011) 462–467, http://dx.doi.org/10.1016/j.bbrc.2011.09.084.
[73] D. Lama, C.J. Brown, D.P. Lane, C.S. Verma, Gating by tryptophan 73 exposes a cryptic pocket at the protein-binding interface of the oncogenic eIF4E protein, Biochemistry 151009161412001 (2015)http://dx.doi.org/10.1021/acs.biochem.5b00812.
[74] I. Rutkowska-Wlodarczyk, J. Stepinski, M. Dadlez, E. Darzynkiewicz, R. Stolarski, A. Niedzwiecka, Structural changes of eIF4E upon binding to the mRNA 5′ monomethylguanosine and trimethylguanosine cap, Biochemistry 47 (2008) 2710–2720, http://dx.doi.org/10.1021/bi701168z.
[75] C. Mazza, A. Segref, I.W. Mattaj, S. Cusack, Large-scale induced fit recognition of an m7GpppG cap analogue by the human nuclear cap-binding complex, EMBO J. 21 (2002) 5548–5557, http://dx.doi.org/10.1093/emboj/cdf538.
[76] R. Worch, A. Niedzwiecka, J. Stepinski, C. Mazza, M. Jankowska-Anyszka, E. Darzynkiewicz, et al., Specificity of recognition of mRNA 5′ cap by human nuclear cap-binding complex. RNA (New York, N.Y.) 11 (2005) 1355–1363, http://dx.doi.org/10.1261/rna.2850705.
[77] R. Worch, M. Jankowska-Anyszka, A. Niedzwiecka, J. Stepinski, C. Mazza, E. Darzynkiewicz, et al., Diverse role of three tyrosines in binding of the RNA 5′ cap to the human nuclear cap binding complex, J. Mol. Biol. 385 (2009) 618–627, http://dx.doi.org/10.1016/j.jmb.2008.10.092.
[78] D. Chagnovich, R. Lehmann, Poly(A)-independent regulation of maternal hunchback translation in the *Drosophila* embryo, Proc. Natl. Acad. Sci. U. S. A. 98 (2001) 11359–11364, http://dx.doi.org/10.1073/pnas.201284398.
[79] J. Marcotrigiano, A.C. Gingras, N. Sonenberg, S.K. Burley, Cap-dependent translation initiation in eukaryotes is regulated by a molecular mimic of eIF4G, Mol. Cell 3 (1999) 707–716, http://dx.doi.org/10.1016/S1097-2765(01)80003-4.